Spin-Orbit-Torque Memory Operation of Synthetic Antiferromagnets

Takahiro Moriyama,[1,2,*] Weinan Zhou,[3] Takeshi Seki,[3,4] Koki Takanashi,[3,4] and Teruo Ono[1,2]
[1]Institute for Chemical Research, Kyoto University, Uji, Kyoto, 611-0011, Japan
[2]Center for Spintronics Research Network, Osaka University, Toyonaka, Osaka, 560-8531, Japan
[3]Institute for Materials Research, Tohoku University, Sendai, Miyagi, 980-8577, Japan
[4]Center for Spintronics Research Network, Tohoku University, Sendai, Miyagi, 980-8577, Japan

(Received 19 June 2018; published 18 October 2018)

In this Letter, we show the demonstration of a sequential antiferromagnetic memory operation with a spin-orbit-torque write, by the spin Hall effect, and a resistive read in the CoGd synthetic antiferromagnetic bits, in which we reveal the distinct differences in the spin-orbit-torque and field-induced switching mechanisms of the antiferromagnetic moment, or the Néel vector. In addition to the comprehensive spin torque memory operation, our thorough investigations also highlight the high immunity to a field disturbance as well as a memristive behavior of the antiferromagnetic bits.

DOI: 10.1103/PhysRevLett.121.167202

Magnetic susceptibilities of antiferromagnetic materials are usually several orders of magnitude smaller than those of ferromagnetic materials [1]. Antiferromagnets are therefore essentially invisible to an external magnetic field. Furthermore, there is no dipole field seeping out of the material since the magnetic moments in antiferromagnets are compensated by each other. These properties give a breakthrough on the memory density when memory bits are packed closer and a bit interference due to the stray field becomes a concern for the conventional ferromagnetic bits [2–7]. Some reports have already suggested that it is possible to control the antiferromagnetic moments by the spin transfer torque [8–12] as well as by the relativistic spin orbit torque [13,14] in a similar principle to that for ferromagnets. The spin torque (ST) control of the magnetization and the immunity to a field disturbance can therefore be reconciled in antiferromagnetic memory bits.

Wadley *et al.* [14] have recently reported that the tetragonal phase CuMnAs having a broken inversion symmetry in its spin sublattices gives rise to the ST by a flow of an electric current in itself. Although their seminal reports [13–15] seem to magnificently advance the memory operation principle of antiferromagnetic bits, the choice of the materials having such a complex unit cell structure is quite limited. To further pave a wide pathway of antiferromagnetic spintronics [2,3], it is desirable to seek the possibility of a universal operation principle of the antiferromagnetic memory.

In this work, we make use of the spin Hall effect [16] to generate a spin current. A variety of architectures based on the spin Hall effect have already been proposed and demonstrated for ferromagnetic memory and logic device applications [17,18]. We show a successful write-read operation of the antiferromagnetic bits made of a multilayer of CoGd amorphous alloys using a spin current generated by the spin Hall effect of Pt as the basic scheme shown in Fig. 1(a), demonstrating a more general antiferromagnetic memory operation principle without relying on the complex crystalline structure.

Multilayers of Pt 4 nm/ $Co_{86}Gd_{14}$6 nm/$Co_{62}Gd_{38}$6 nm/ Pt 4 nm (sample #1) and $Co_{86}Gd_{14}$6 nm/$Co_{62}Gd_{38}$6 nm/ Pt 4 nm (sample #2) were prepared on a thermally oxidized Si substrate by magnetron sputtering. The CoGd alloys were formed by codeposition of Co and Gd at room temperature with a base pressure below 1×10^{-7} Pa. Composition of the CoGd alloy was determined by electron probe x-ray microanalysis. CoGd amorphous alloys are a well-known ferrimagnet in which the Gd and the Co moment are antiferromagnetically coupled [19]. Therefore, one can tune the size of the net magnetization by Co and Gd compositions. Alternatively, the size of the net magnetization can also be controlled by temperature as the size of the Gd moment changes significantly with temperature. In our experiments, we used a bilayer of the different composition CoGd layers so that, at a certain temperature, we can synthetically realize an antiferromagnet in which the net magnetizations in the two CoGd layers are antiferromagnetically coupled with zero total magnetization as shown in Fig. 1(b) (see Supplemental Material for detail [20,21].). In order to demonstrate the memory operation, the multilayers were patterned into a Hall cross structure shown in Fig. 1(c). We measured both the sheet resistance (R_{sheet}) and the Hall resistance (R_{Hall}) using a multiplexer system.

In the following, we show the results of the ST writing and compare them with the results of the complemental field writing. Figure 1(d) describes the ST writing scheme. A current flowing from electrode 2 and 4 to electrode 1 and 3 writes "0." A current flowing from electrode 2 and 3 to electrode 1 and 4 writes "1." For instance, considering

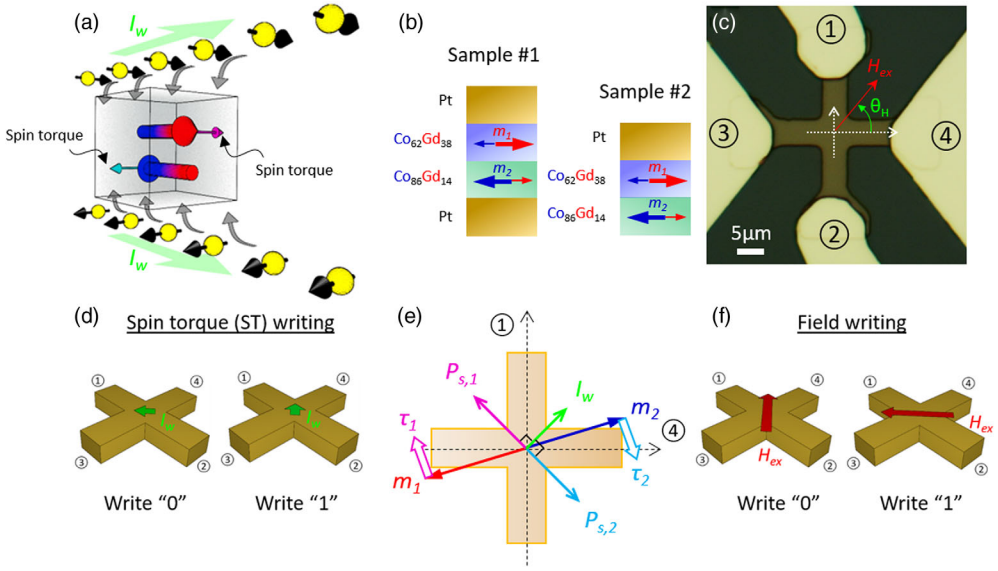

FIG. 1. The spin torque (ST) writing scheme and the samples. (a) The basic scheme of the ST rotation of the antiferromagnet using the spin Hall effect. The writing current I_w invokes the spin Hall effect, and injects the spin currents toward the antiferromagnetic bit. The spin torques rotate the magnetizations in the same rotation direction. (b) Layer stacks of sample #1 consisting of a thermally oxidized Si substrate/ Pt 4 nm/ $Co_{86}Gd_{14}$6 nm/$Co_{62}Gd_{38}$6 nm/ Pt 4 nm and sample #2 consisting of a thermally oxidized Si substrate/ $Co_{86}Gd_{14}$6 nm/$Co_{62}Gd_{38}$6 nm/ Pt 4 nm. The blue and red arrows represent the Co and Gd moments, respectively. m_1 and m_2 are the net magnetization in each layer. (c) Microscope image of the Hall cross structure. Electrodes labeled with 1–4 are made of Ti 5 nm/Au 100 nm. Definition of the field angle θ_H is also indicated. (d) The ST writing scheme. The directions of current flow up on writing "0" and "1" are presented. (e) Vectors of the net writing current I_w, polarization of the spin current $P_{s,1}$ and $P_{s,2}$, magnetizations in the CoGd layers m_1 (top) and m_2 (bottom), and the ST acting on the magnetizations τ_1 and τ_2 when considering sample #1. (f) The field writing scheme. The directions of the external field up on writing "0" and "1" are presented.

sample #1, due to the spin Hall effect of the top and the bottom Pt layers, the net current I_w to write "1" generates the spin currents with their polarizations orthogonal to the direction of the net current flow as described in Fig. 1(e) where $\boldsymbol{P}_{s,1}$ and $\boldsymbol{P}_{s,2}$ represent the polarization of the spin current from the top and the bottom Pt layers, respectively. These spin currents exert a spin torque $\boldsymbol{\tau}_1 \propto \boldsymbol{m}_1 \times \boldsymbol{P}_{s,1} \times \boldsymbol{m}_1$ and $\boldsymbol{\tau}_2 \propto \boldsymbol{m}_2 \times \boldsymbol{P}_{s,2} \times \boldsymbol{m}_2$ on the magnetization of the top ($\boldsymbol{m}_1$) and the bottom ($\boldsymbol{m}_2$) CoGd layers, respectively. Consequently, $\boldsymbol{\tau}_1$ and $\boldsymbol{\tau}_2$ rotate $\boldsymbol{m}_1$ and $\boldsymbol{m}_2$ in the same rotation direction and the magnetizations are stabilized when they are in the same direction as $\boldsymbol{P}_{s,1}$ and $\boldsymbol{P}_{s,2}$. The writing operation therefore directs the magnetizations perpendicular to the direction of the writing current. The state "0" and "1" are read by a change of R_{Hall} due to the planar Hall effect. For our switching measurements, I_w was applied for a duration of 6 sec and then R_{Hall} was read multiple times with an interval of 30 sec. The "measurement count" in the switching results (e.g., Fig. 3) represents each reading. Figure 1(f) describes the field writing complementally performed in our experiment. An in-plane external field H_{ex} is applied at $\theta_H = 45°$ and $\theta_H = 135°$ [see Fig. 1(c) for the definition of θ_H] which, respectively, writes "0" and "1." More detailed descriptions on these measurement schemes can be found in the Supplemental Material [20,21]].

We first determine the magnetic state of the samples by measuring R_{Hall} in a rotating in-plane magnetic field. Figure 2(a) shows R_{Hall} as a function of θ_H in sample #1 at various temperatures (see also the R_{sheet} profiles in Supplemental Material [20,21]). We applied a constant external field of $H_{\mathrm{ex}} = 3$ kOe. At $T = 312$ and 254 K, R_{Hall} shows a $1 - \sin 2\theta_H$ function indicating the total magnetization of the sample is pointing in the same direction as H_{ex} [see Fig. 2(b)]. On the other hand, at $T = 283$ K, the R_{Hall} profile shifts by $\theta_H = \pi/2$, indicating that the total magnetization becomes zero (becomes antiferromagnetic) and the two magnetizations of the CoGd layers are now perpendicular to the external field in order to reduce the Zeeman energy as well as the exchange energy as described in Fig. 2(c). We call this temperature the magnetization compensation temperature (T_c) in the following discussion. In the same manner, we also estimate T_c of sample #2 to be 256 K. The slight difference in T_c in the two samples may originate from the layer growth quality of the CoGd with and without a presence of the bottom Pt layer.

Figure 3 shows the results of the ST writing and the field writing of sample #1 at various temperatures (see Supplemental Material [20,21] for comprehensive data). The ST writing and the resistive reading are clearly successful at T_c as shown in Fig. 3(a). R_{Hall} becomes a

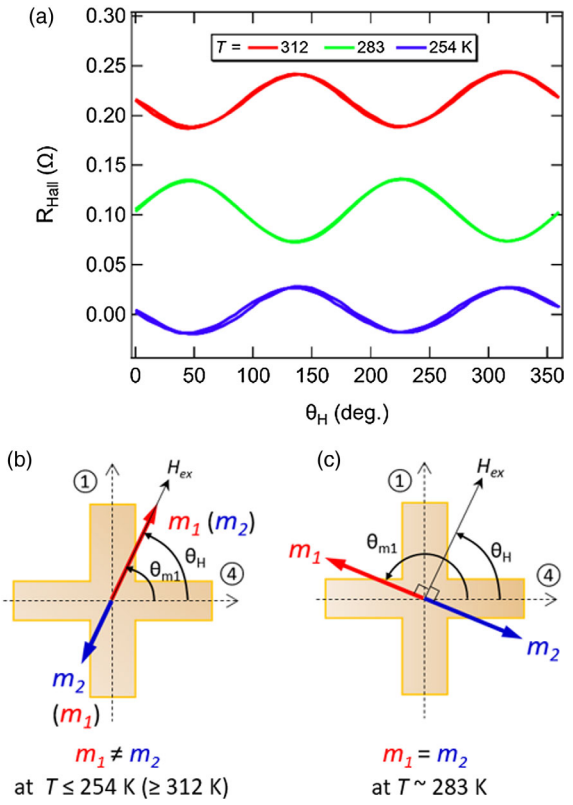

FIG. 2. Electrical resistance measurements in a rotating in-plane magnetic field. (a) The Hall resistance R_{Hall} as a function of θ_H with $H_{\mathrm{ex}} = 3$ kOe at various temperatures. R_{Hall} curves are offset for visibility. Rotation of magnetizations with respect to the rotating H_{ex} direction (b) at $T \neq T_c$ and (c) at $T = T_c$. The net magnetizations of m_1 and m_2 are always either parallel or antiparallel to the rotating H_{ex} at $T \neq T_c$, while magnetizations m_1 and m_2 are always perpendicular to the rotating H_{ex} at $T = T_c$.

high state after writing "1", which implies that the magnetization directions are set perpendicular to I_w [referring to Fig. 2(a), it is the same situation when the external field is applied at $\theta_H = 45°$ at T_c]. It is noteworthy that even at $T \neq T_c$, the temperatures at which the sample becomes ferrimagnetic, the ST writing current successfully rotates the magnetizations $\mathbf{m_1}$ and $\mathbf{m_2}$ as seen in Fig. 3(c). This indicates that the operation principle described in Fig. 1(e) is effective even for the ferrimagnetic state since the spin current from the Pt layer most probably exerts a spin torque only on the adjacent CoGd layer. Contrary to the ST writing, the field writing and the resistive reading at $T = T_c$ are not as clear [Fig. 3(b)]. We observed only a small change of R_{Hall} after each writing operation, which proves that the antiferromagnetic memory bits are indeed immune to an external field. Note that with $H_{\mathrm{ex}} = 4$ kOe the resistance low-high trend is reversed, suggesting that the magnetizations are spin flopped and, consequently, they point perpendicular to the writing field. At $T \neq T_c$, the R_{Hall} response after the field writing [Fig. 3(d)] simply indicates that the total magnetization rotates in the direction of the writing field. We note that both of the ST and the field write-read results are found irrelevant to the polarity of the current and the field.

In addition to the normal memory writing tests described above, we conducted the continuous writing with the ST write "0" as well as the write "1." The results for sample #1 are shown in Figs. 3(e) and 3(f). The continuous ST writing keeps changing R_{Hall} to a low value for write "0" and a high value for write "1" and R_{Hall} then shows a saturation. This accumulative change of R_{Hall} with respect to the amount of current flow is nothing but a memristive behavior which is recently researched actively for neuromorphic devices [22,23]. We find that this asymptotic R_{Hall} behavior is well fitted with an exponential decay function. The saturated value $\Delta R_{\mathrm{Hall,sat}}$, considered the full change of R_{Hall} up on the ST writing, is extracted by extrapolating the decay functions.

Concerning a future memory architecture with a magnetic tunnel junction structure to enhance the read signal, it is important to leave one of the surfaces for a tunnel barrier contact [24]. We foresee sample #2 could be more suitable in this regard. The results of write-read tests and the memrisitve behavior turn out to be quite similar to those of sample #1 (see Supplemental Material [20,21]).

Figure 4 summarizes ΔR_{Hall} (change of R_{Hall} after each writing operation indicated in Fig. 3) with various strengths of the writing current and field for Sample #1 and #2. For the ST writing (Fig. 4(a) and 4(c)), larger I_w induces larger ΔR_{Hall} and it also shows a threshold. At $T = T_c$, the threshold current is about 10 mA which corresponds to the current density of 7×10^6 A/cm^2 for Sample #1 and is about 7 mA corresponding to 6×10^6 A/cm^2 for Sample #2. For the field writing (Fig. 4(b) and 4(d)), ΔR_{Hall} is almost insensitive to the writing at $T = T_c$, while it saturates above 1.5 kOe for $T \neq T_c$. The negative ΔR_{Hall} at $T = T_c$ with a high writing field (see the green plots in Fig. 4(b) and 4(d)) is a consequence of the spin flopping. It is important to note that the ST writing induces ΔR_{Hall} by only a fraction of ΔR_{Hall} (~32 mΩ and ~17 mΩ for samples #1 and #2, respectively) induced by the field writing. This essentially implies that a single ST writing rotates the magnetizations in only a portion, maybe as a domain, of the sample at a time.

In Fig. 5, we plot $\Delta R_{\mathrm{Hall,sat}}$ induced by ST writing and ΔR_{Hall} induced by the field writing with respect to temperature for samples #1 and #2. The plots clearly represent the excellence of the antiferromagnetic memory bit, i.e., the robustness against the field disturbance and the capability of the ST manipulation [25] (Also see Supplemental Material [20,21] for further discussion.). While the ST writing is always effective regardless of the temperature in sample #1, it seems that the ST becomes less effective to the rotation of the magnetizations at $T \neq T_c$ in sample #2. This may indicate that, when the spin current is applied from one side, the ST efficiency depends on the size of the total

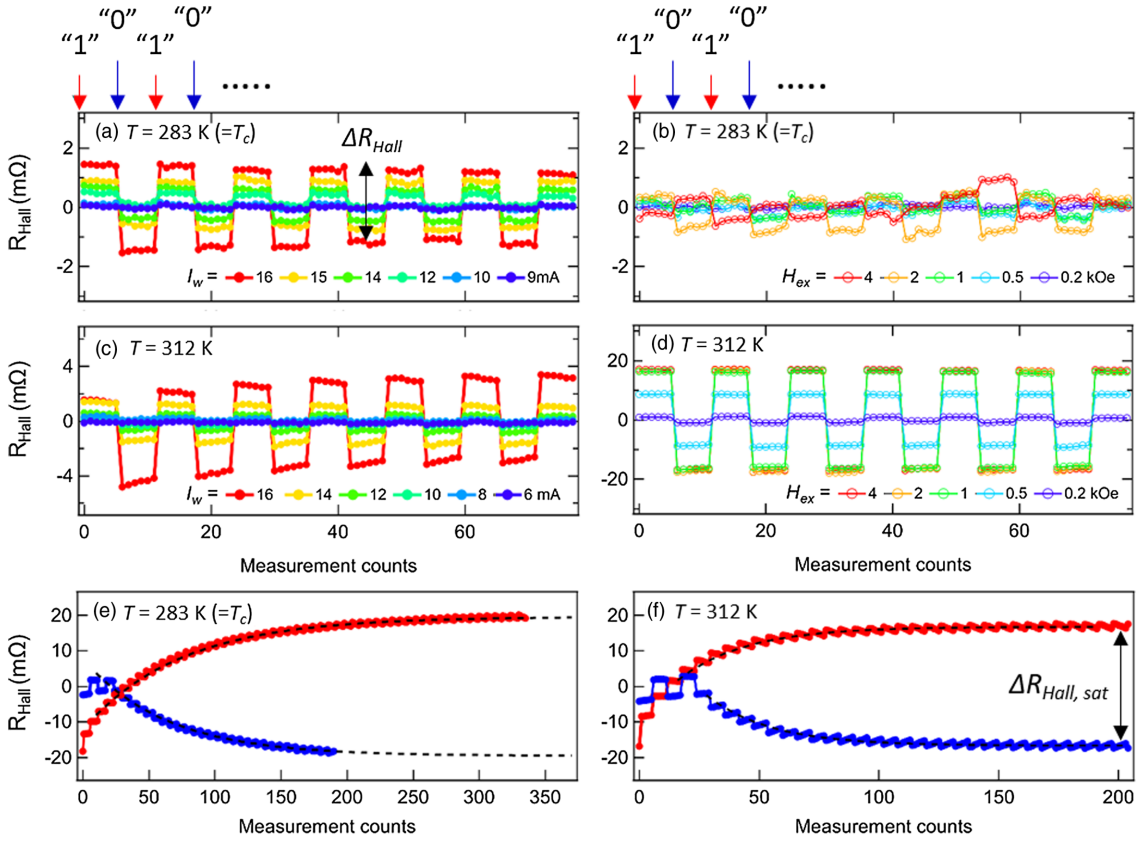

FIG. 3. Sequential write and read operation for sample #1. (a), (b), and (e) show the results of the ST write-read, the field write-read, and the continuous ST write-read, respectively, at $T = 283$ K ($=T_c$). (c), (d), and (f) show the results of the ST write-read, the field write-read, and the continuous ST write-read, respectively, at $T = 312$ K. The arrows on the top represent the write "1" and "0" operations described in Figs. 1(d) and 1(f). As indicated in the graph, ΔR_{Hall} is defined as $\Delta R_{\mathrm{Hall}} = R_{\mathrm{Hall}}(\text{"1"}) - R_{\mathrm{Hall}}(\text{"0"})$ where R_{Hall} ("1") and R_{Hall} ("0") represent the R_{Hall} after the write "1" and the write "0", respectively. For the continuous write-read tests, the blue and the red plot represent the continuous ST write "0" and the continuous write "1" operation, respectively, with $I_w = 16$ mA. Note that the first 2 cycles of the blue data plot show a normal "0" → "1" writing operation. The dotted curves are the fitting with an exponential decay function $y = y_0 + Ae^{-[(x+x_0)/\tau]}$. $\Delta R_{\mathrm{Hall,sat}}$, indicated in (f), is determined by extrapolating the decay functions.

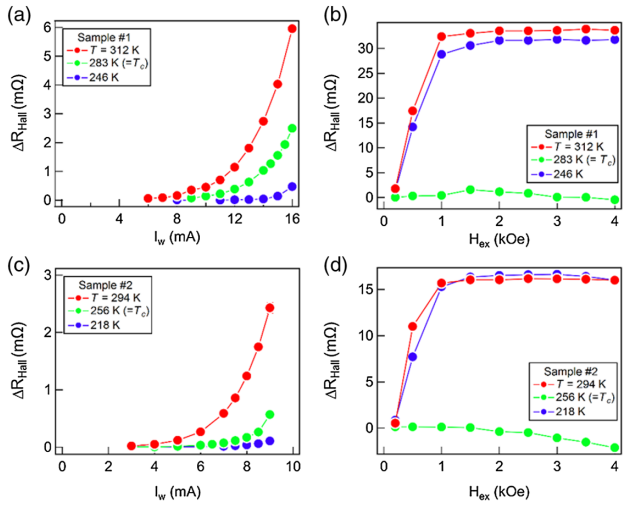

FIG. 4. I_w and H_{ex} dependence of ΔR_{Hall}. ΔR_{Hall} as a function of the writing current I_w (a) and the writing field H_{ex} (b) for sample #1 at various temperatures and ΔR_{Hall} as a function of the writing current I_w (c) and the writing field H_{ex} (d) for sample #2 at various temperatures.

magnetizations of the sample. The comparison between the ST and the field writing for sample #2 at $T = T_c$ [see Fig. 5(b)] clearly dictates the rotation of the magnetizations are predominantly driven by the ST not by the emerging

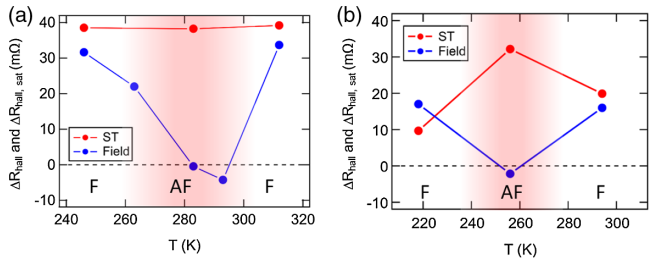

FIG. 5. Summary of the ST and the field writing. $\Delta R_{\mathrm{Hall,sat}}$ by the ST writing (red) and the ΔR_{Hall} by the field writing (blue) as a function of temperature for sample #1 (a) and sample #2 (b). The presented values of ΔR_{Hall} by the field writing are taken from the data shown in Fig. 4 at $H_{\mathrm{ex}} = 4$ kOe. The temperature range where the sample becomes antiferromagnetic (AF) is indicated in the red area. Outside the temperature range, the sample is ferrimagnetic (F).

field created by the current flow (e.g., the Oersted field or other fieldlike torques). It should be emphasized that the experimental results essentially prove that $\boldsymbol{\tau}_{1,2} \propto \boldsymbol{m}_{1,2} \times \boldsymbol{P}_{s,1,2} \times \boldsymbol{m}_{1,2}$ directs magnetization rotation and stabilizes it in our writing scheme and $\boldsymbol{H}_{\mathbf{eff},1,2} \propto \boldsymbol{m}_{1,2} \times \boldsymbol{P}_{s,1,2}$ the direction of which is perpendicular to the sample plane is less relevant in this case [11,12].

In summary, we demonstrated a ST memory operation principle with antiferromagnetic bits made of CoGd amorphous alloys. We have successfully written the antiferromagnetic bits using the ST generated by the spin Hall effect and read the written magnetic state by the resistance. By comparing with the complemental field writing tests, we revealed the clear differences in ST and field switching mechanisms and also showed that the antiferromagnetic bits were immune to an external field disturbance. The ST switching seems to occur in a portion of the antiferromagnetic bit at a time, leading to the memristive behavior which may be useful for the neuromorphic applications. We also implicate that our architecture and operation principle will well be used in practical memory devices as it, in the case of sample #2, can be implemented with a general process of making a magnetic tunnel junction to enhance the resistive signal. Finally, we remark that the universal operation principle of the ST antiferromagnetic memory is now ready for next generation spintronic devices.

This work was supported by JSPS KAKENHI Grants No. 15H05702, No. 26870300, No. 17H04924, No. 17H05181, and No. 16H04487.

*Corresponding author.
mtaka@scl.kyoto-u.ac.jp

[1] L. Néel, in *Nobel Lectures, Physics 1963-1970* (Elsevier Publishing Company, Amsterdam, 1972), p. 318.
[2] T. Jungwirth, X. Marti, P. Wadley, and J. Wunderlich, Nat. Nanotechnol. **11**, 231 (2016).
[3] V. Baltz, A. Manchon, M. Tsoi, T. Moriyama, T. Ono, and Y. Tserkovnyak, Rev. Mod. Phys. **90**, 015005 (2018).
[4] S. Loth, S. Baumann, C. P. Lutz, D. M. Eigler, and A. J. Heinrich, Science **335**, 196 (2012).
[5] X. Marti, I. Fina, C. Frontera, J. Liu, P. Wadley, Q. He, R. J. Paull, J. D. Clarkson, J. Kudrnovský, I. Turek, J. Kuneš, D. Yi, J. Chu, C. T. Nelson, L. You, E. Arenholz, S. Salahuddin, J. Fontcuberta, T. Jungwirth, and R. Ramesh, Nat. Mater. **13**, 367 (2014).
[6] T. Moriyama, N. Matsuzaki, K.-J. Kim, I. Suzuki, T. Taniyama, and T. Ono, Appl. Phys. Lett. **107**, 122403 (2015).
[7] D. Kriegner, K. Výborný, K. Olejník, H. Reichlová, V. Novák, X. Marti, J. Gazquez, V. Saidl, P. Němec, V. V. Volobuev, G. Springholz, V. Holý, and T. Jungwirth, Nat. Commun. **7**, 11623 (2016).
[8] P. M. Haney and A. H. MacDonald, Phys. Rev. Lett. **100**, 196801 (2008).
[9] H. V. Gomonay and V. M. Loktev, Phys. Rev. B **81**, 144427 (2010).
[10] T. Moriyama, M. Kamiya, K. Oda, K. Tanaka, K.-J. Kim, and T. Ono, Phys. Rev. Lett. **119**, 267204 (2017).
[11] T. Moriyama, K. Oda, and T. Ono, arXiv:1708.07682.
[12] X. Z. Chen, R. Zarzuela, J. Zhang, C. Song, X. F. Zhou, G. Y. Shi, F. Li, H. A. Zhou, W. J. Jiang, F. Pan, and Y. Tserkovnyak, Phys. Rev. Lett. **120**, 207204 (2018).
[13] J. Železný, H. Gao, K. Výborný, J. Zemen, J. Mašek, A. Manchon, J. Wunderlich, J. Sinova, and T. Jungwirth, Phys. Rev. Lett. **113**, 157201 (2014).
[14] P. Wadely *et al.*, Science **351**, 587 (2016).
[15] M. J. Grzybowski, P. Wadley, K. W. Edmonds, R. Beardsley, V. Hills, R. P. Campion, B. L. Gallagher, J. S. Chauhan, V. Novak, T. Jungwirth, F. Maccherozzi, and S. S. Dhesi, Phys. Rev. Lett. **118**, 057701 (2017).
[16] M. I. Dyakonov and V. I. Perel, Sov. Phys. JETP Lett. **13**, 467 (1971).
[17] L. Liu, C.-F. Pai, Y. Li, H. W. Tseng, D. C. Ralph, and R. A. Buhrman, Science **336**, 555 (2012).
[18] S. Emori, U. Bauer, S.-M. Ahn, E. Martinez, and G. S. D. Beach, Nat. Mater. **12**, 611 (2013).
[19] P. Chaudhari, J. J. Cuomo, and R. J. Gambino, Appl. Phys. Lett. **22**, 337 (1973).
[20] See Supplemental Material at http://link.aps.org/supplemental/10.1103/PhysRevLett.121.167202 for extended data sets and discussions, which includes Ref. [21].
[21] S. Chikazumi, *Physics of Ferromagnetism* (OUP Oxford, New York, 2009).
[22] D. B. Strukov, G. S. Snider, D. R. Stewart, and S. R. Williams, Nature (London) **453**, 80 (2008).
[23] S. Fukami, C. Zhang, S. DuttaGupta, A. Kurenkov, and H. Ohno, Nat. Mater. **15**, 535 (2016).
[24] B. G. Park, J. Wunderlich, X. Martí, V. Holý, Y. Kurosaki, M. Yamada, H. Yamamoto, A. Nishide, J. Hayakawa, H. Takahashi, A. B. Shick, and T. Jungwirth, Nat. Mater. **10**, 347 (2011).
[25] It is immune to a linear field disturbance. However, it is obviously not the case with a rotating magnetic field as indicated by the result shown in Fig. 3(a).